

200635020A

厚生労働科学研究費補助金

労働安全衛生総合研究事業

斜面崩壊による労働災害防止に関する研究

平成 18 年度 総括研究年度終了報告書

主任研究者 三田地 利之

平成 19 (2007) 年 4 月

## 目次

I. 総括研究年度終了報告	
斜面崩壊による労働災害防止に関する研究	----- 3
三田地 利之	
II. 分担研究年度終了報告書	
1. 斜面崩壊による労働災害防止に関する研究	----- 5
田中洋行	
2. 斜面崩壊による労働災害防止に関する研究	-----6
豊澤康男	
3. 斜面崩壊による労働災害防止に関する研究	-----8
伊藤和也	
III. 研究成果の刊行に関する一覧表	-----10
IV. 研究成果の刊行物・別刷	

厚生労働科学研究費補助金（労働安全衛生総合研究事業）

（総括）研究年度終了報告書

斜面崩壊による労働災害防止に関する研究

主任研究者 三田地 利之 北海道大学 大学院 教授

研究要旨：斜面崩壊による労働災害を防止するために、斜面崩壊の防止、および発生の予知に関する研究を行った。当該年度は、斜面崩壊の予知に向けた掘削中の斜面変位の計測システムの評価および降雨による斜面地盤の地下水位の上昇の検知、さらに地盤強度の評価に関する基礎的研究として、粘性土の引張り強度および残留状態強度に関する研究を行った。

#### A. 研究目的

斜面崩壊による事故防止を目的に、崩壊防止およびその予知についての研究を行う。

#### B. 研究方法

斜面崩壊予知システムの確立に向けて、重力場および遠心場での室内実験ならびに現場実験によって斜面変位の計測システムの評価を行なった。また、遠心場で模型地盤に降雨を発生させ、斜面地盤内の間隙水圧の挙動を調べた。さらに、新規開発の引張り試験装置を用いて、粘性土の引張り強度とサクシオンとの関係を調べた。また、共焦点レーザー走査蛍光顕微鏡を用いたせん断面の観察等を通じて、粘土の残留状態強度の発生メカニズムについて調べた。

#### C. 研究結果

掘削時の斜面崩壊直前の変形状況を直接計測できる傾斜計を開発し、斜面深度方向に間隔を空け連続的に埋めて室内実験を行い、この傾斜計により深度方向の動きを測定可能であることを確認した。さらに、斜面地盤の密度の違いによって、斜面崩壊時

の塑性領域の発生形態が異なることを見出すことができた。また、遠心掘削装置を用い、遠心場で崩壊に至るまで模型斜面の法尻の掘削を行った。実験結果に基づいて、崩壊高さを限界崩壊高さで正規化し、各種の土について検討した結果、地盤の種類によらず正規化曲線の傾きは類似していることが分かった。遠心場での降雨実験では、降雨強度と地下水位の上昇速度との関係を把握することができた。

一方、新たに開発した引張り試験装置にて飽和粘土供試体の引張り強度とサクシオンの関係を測定し、飽和土の試料では引張り強度の値が最大になるときにサクシオンの値もほぼ最大値を示すことが分かった。

さらに、粘土の残留状態せん断抵抗角と真実接触面で発現される摩擦係数との関係を検討し、その考察にもとづいて地すべり対策工設計用強度パラメータの決定法の提案を行った。

#### D. 健康危機情報

なし

## E. 研究発表

### 1. 論文発表

なし

### 2. 学会発表

Possible use of Tilt-sensor for failure movement and failure plane just before slope failure : International Geotechnical symposium on “Geotechnical Engineering for disaster prevention and reduction”, Russia.

Comparison of Failure Mechanism due to Toe Excavation: Field test, Centrifuge test and Numerical Analysis, Geotech Week Symposium, Singapore.

遠心力載荷実験による降雨時の斜面安定の検討：降雨時の斜面モニタリング技術とリアルタイム崩壊予測に関するシンポジウム

Factors affecting tensile strength measurement and Modified Tensile Strength measuring apparatus for soil : Mechanics of Unsaturated soils, Weimar, Germany.

粘土の残留状態におけるせん断抵抗係数  $\tan \phi' r$  と真実接触面積との関係：地盤工学会北海道支部技術研究発表会.

粘土の残留強度と地すべり対策工設計用強度：日本地すべり学会北海道支部特別講演.

### 3. シンポジウムの開催

中央労働災害防止協会の「労働安全衛生総合研究成果発表会支援事業により、「斜面崩壊による災害防止に関するシンポジウム」を開催し、主任研究者および分担研究者の研究成果に加えて、本テーマに関わる内外の研究者の研究成果に関する情報交換の場を設けるとともに、発表内容を収録した論文集（別添）を発行した.

## F. 知的財産権の出願・登録状況

### 1. 特許取得

小型自動繰り返し一面せん断試験装置

（特許 第 379521 号, 2006 年 4 月）

アーム可動型遠心力載荷試験装置

（特許 第 3878093 号, 2006 年 11 月）

### 2. 実用新案登録

なし

### 3. その他

なし

厚生労働科学研究費補助金 (労働安全衛生総合研究事業)

(総括) 研究年度終了報告書

斜面崩壊による労働災害防止に関する研究

分担研究者 田中 洋行 北海道大学 大学院 助教授

研究要旨：斜面崩壊による労働災害を防止するために、斜面崩壊の防止、および発生の予知に関する研究を行った。当該年度は、透水係数が異なる斜面地盤について降雨による地下水位の上昇に関する研究を行った。

A 研究目的

斜面崩壊の事故を防止するために、降雨による崩壊のメカニズム、およびその予知についての研究を行う。

B 研究方法

降雨による斜面崩壊のメカニズムを明らかにするために、遠心力载荷実験において、透水性の異なる模型地盤を作成し、不飽和土における降雨による地中の間隙水圧の挙動について調べた。

C 研究結果

遠心力を平面および斜面地盤に負荷し、降雨を与えることにより、地盤内の地下水位上昇を捉えた。実験は降雨強度と遠心力を変化させ、地下水位の上昇速度との関連の把握を試みた。

地盤の透水性が低下すると、地下水面より上の地盤では大きなサクションが作用する。また、降雨開始から地盤内の間隙水圧上昇までにタイムラグが大きくなる傾向が得られた。遠心力载荷実験では、模型地盤を縮小しても、地盤内に作用している応力状態は実物と同じにできる利点がある。その代わりに、模型と実物との相似則を明らかにする必要がある。この相似則を

確立するために、降雨強度と G を変化させて実験を行った。

D 健康危機情報

なし

E 研究発表

1. 論文発表

なし

2. 学会発表

遠心力载荷試験による降雨時の斜面安定の検討:降雨時の斜面モニタリング技術とリアルタイム崩壊予測に関するシンポジウム

遠心場における降雨再現実験での間隙水圧の挙動：地盤工学会北海道支部

遠心模型実験を用いた降雨再現実験での間隙水圧の挙動：地盤工学会全国大会

F 知的財産権の出願・登録状況

1. 特許取得

なし

2. 実用新案登録

なし

3. その他

なし

厚生労働科学研究費補助金 (労働安全衛生総合研究事業)

(総括) 研究年度終了報告書

斜面崩壊による労働災害防止に関する研究

分担研究者 豊澤康男 独立行政法人産業安全研究所 統括研究員

研究要旨：斜面崩壊による労働災害を防止するために，斜面崩壊の防止，および発生の予測・検知に関する研究を行った。当該年度は，簡易に計測できる高精度傾斜計について中規模実験および実物大実験を行った。

#### A 研究目的

斜面崩壊での労働災害を防止するために，崩壊の予測・検知システムを開発することを目的として，簡易に設置・計測が出来る高精度傾斜計の開発・試作とそれを用いた実験を行い，その性能を検証した。

#### B 研究方法

斜面崩壊での変化を確認するために，高さ 1~2m の砂質土斜面と高さ 5m の砂質土・粘性土斜面を作成して斜面崩壊実験を行った。実験は，急傾斜対策工事や道路拡張工事の際に使用される重力式擁壁を施工する際に行われる床掘りを段階的に行った。斜面天端と斜面上部に高精度傾斜計を設置し崩壊までの挙動を計測した。

#### C 研究結果

ここでは，高さ 5m の砂質土斜面にて行った斜面崩壊実験の結果について説明する。実験は密に締め固めた斜面と緩く締め固めた斜面の 2 種類で行い，崩壊挙動の違いについて確認した。実験では，斜面上部に 2 つ，天端に 3 つの傾斜計を設置した。この傾斜計は斜面の前後方向の傾斜を計測しており，前方に傾斜した場合はプラス，後方に傾斜した場合はマイナスで角度が

出力されるようになっている。緩い締め固めの斜面では，掘削に伴い全ての傾斜計が斜面の前方に向かって傾斜した。また崩壊直前において，法肩から最長距離に設置してある傾斜計を除いて，傾斜の増加が著しくなった。密に締め固められた斜面においても，崩壊直前において，緩く締め固められた斜面同様の傾斜の増加傾向を確認できた。しかしながら，角度の出力方向に着目してみると，天端内の傾斜計は緩く締め固められた斜面と同様に，全てが斜面の前方に傾斜しているが，斜面内の傾斜計は斜面の後方に向かって傾く結果となった。これらのことから，緩い斜面では，掘削の進行に伴い塑性領域が天端に向かって増加し，斜面が前方に向かって崩壊する傾向を示し，密な斜面では，掘削の進行に伴い掘削面下部に局所的な塑性領域が，天端には広く引張応力が発生して，斜面部は斜面後方に，天端部は斜面前方に向かって崩壊するという崩壊メカニズムを指摘できる。

今後，これらの結果を元にして崩壊の判定基準等の設定を検討したいと考えている。

#### D 健康危機情報

なし

E 研究発表

1. 論文発表

なし

2 学会発表

Development of Tilt-sensor and possibility of measurement of failure trend just before the failure : 平成 18 年度地盤工学研究発表会

Development of Tilt-sensor for advance prediction of failure and its applicability in the field excavation : 第 36 回安全工学シンポジウム

Relationship between critical failure height and trench excavation depth in relation to centrifuge tests performed with In-flight excavator : 第 36 回安全工学シンポジウム

Comparison of slope failure trend just before failure in the field using newly developed tilt-sensor : 土木学会第 61 回年次学術講演会

Comparison of failure heights during excavation of slope using In-flight excavator : The 6th International Conference on Physical Modelling in Geotechnics 2006(Hong Kong)

Comparison Failure Mechanism due to Toe Excavation: Centrifuge, Field Tests and Numerical Analyses , 1st Geotechnique, CI-Premier conference, Singapore.

Possibility of measurement of slope movement during the sandy soil slope failure in centrifuge : Sea to Sky Geotechnique 2006

F 知的財産権の出願・登録状況

1 特許取得

なし

2 実用新案登録

なし

3 その他

なし

厚生労働科学研究費補助金 (労働安全衛生総合研究事業)

(総括) 研究年度終了報告書

斜面崩壊による労働災害防止に関する研究

分担研究者 伊藤和也 独立行政法人労働安全衛生総合研究所 研究員

研究要旨：斜面崩壊による労働災害を防止するために、斜面崩壊の防止、および発生の予測・検知に関する研究を行った。当該年度は、掘削方法による斜面崩壊メカニズムの影響と、斜面の崩壊可能性を判断するための原位置試験機の開発・試作を行った。

#### A 研究目的

斜面崩壊での労働災害を防止するために、崩壊の予測・検知システムを開発することを目的として、掘削方法による斜面崩壊メカニズムの影響について研究を行った。

また、斜面の崩壊可能性を判断する手段として、現場にて簡易に地盤強度を測定することが出来る簡易静的コーン貫入試験機の開発を行った。

#### B 研究方法

掘削方法による斜面崩壊メカニズムの影響を確認するために遠心模型実験装置を用いて斜面地盤を再現し、掘削方法を変化させた実験を行った。実験は急傾斜対策工事や道路拡張工事の際に使用される重力式擁壁を施工する際に行われる床掘りの場所を変化させた。試料は、砂質系試料として成田砂を、粘性土系試料として関東ロームを使用した。また、斜面上部に変位計を設置することで鉛直変位を計測した。遠心加速度は 31G とし、遠心場掘削装置を用いて段階的に掘削を行った。

#### C 研究結果

法面だけを掘削した場合と、法面掘削の際に床掘りも掘削した方法による崩壊高さの違いについて比較した。その結果、法面掘削の際に床掘りも掘削を行うと、法面掘削だけの場合と比べて崩壊する高さが低くなる傾向が得られた。これは、斜面が崩壊する際に影響を与える土塊重量のバランスの問題だと考えられる。すなわち、床掘り掘削は、その土塊重量が法面掘削に比べて低い掘削高さで大きくなる可能性が高いことが指摘でき、床掘り掘削の際には注意が必要であることが分かった。また、斜面上部に取り付けた変位計の挙動から、斜面に近い箇所に取り付けた変位計の沈下量が崩壊直前に急激に増加しており、崩壊域にて変位計測を行うことで、崩壊の予測が可能ではないかと思われた。

斜面の崩壊可能性を判断する手段として、現場にて簡易に地盤強度を測定することが出来る簡易静的コーン貫入試験機を開発し、試作機を製作した。今後、その性能を確認する予定である。

#### D 健康危機情報

なし



E 研究発表

1. 論文発表

なし

2 学会発表

Development of Tilt-sensor and possibility of measurement of failure trend just before the failure : 平成 18 年度地盤工学研究発表会

Development of Tilt-sensor for advance prediction of failure and its applicability in the field excavation : 第 36 回安全工学シンポジウム

Relationship between critical failure height and trench excavation depth in relation to centrifuge tests performed with In-flight excavator : 第 36 回安全工学シンポジウム

Comparison of slope failure trend just before failure in the field using newly developed tilt-sensor : 土木学会第 61 回年次学術講演会

excavation of slope using In-flight excavator : The 6th International Conference on Physical Modelling in Geotechnics 2006(Hong Kong)

Comparison of failure heights during excavation of slope using In-flight excavator : The 6th International Conference on Physical Modelling in Geotechnics 2006(Hong Kong)

Comparison Failure Mechanism due to Toe Excavation: Centrifuge, Field Tests and Numerical Analyses : 1st Geotechnique, CI-Premier conference, Singapore.

Possibility of measurement of slope movement during the sandy soil slope failure in centrifuge : Sea to Sky Geotechnique 2006

F 知的財産権の出願・登録状況

1 特許取得

なし

2 実用新案登録

なし

3 その他

なし

## 研究成果の刊行に関する一覧表

発表者名：“論文タイトル名”，発表誌名，巻号，ページ，出版年

### 1. 国際学会・シンポジウム等

Tamrakar S.B., Toyosawa Y., Itoh K. & Timpong S.: Failure heights during excavation of slope using In-flight excavator, International conference on Physical Modeling in Geotechnics - 2006, Physical Modeling in Geotechnics-6th ICPMG 2006, Ng, Zhang and Wang (eds), Vol. 1, pp. 385 - 390, ISBN 0-415-41586-1, 2006.

Tamrakar S.B., Toyosawa Y., Tanaka H. and Itoh K.: Possibility of measurement of slope movement during the Sandy soil slope failure in centrifuge, Sea to Sky Geotechnique-2006, 59th Canadian Geotechnical Conference, pp. 351-358, 2006.

Timpong S., Toyosawa Y., Tamrakar S.B., Miura S. and Itoh K.: Investigation of slope failure during trench excavation in peat ground, 59th Canadian Geotechnical Conference, Sea to Sky Geotechnique, Vancouver, Canada, pp. 389 - 393, 2006.

Toyosawa Y., Yang J., Timpong S., Itoh K. and Tamrakar S. B.: Stability of Trench Excavation under Construction Machinery Load, 59th Canadian Geotechnical Conference, Sea to Sky Geotechnique, Vancouver, Canada, pp. 376 - 381, 2006.

Tamrakar S.B., Toyosawa Y., Itoh K. and Mitachi T.: Comparison of Failure Mechanism due to Toe Excavation: Field test, Centrifuge test and Numerical Analysis, Geotech Week Symposium, Singapore, 2006.

Tamrakar S.B., Mitachi T. and Toyosawa Y.: Factors affecting tensile strength measurement and Modified Tensile Strength measuring apparatus for soil, Mechanics of Unsaturated soils, Weimar, Germany, 2007. (in print)

Tamrakar S.B., Toyosawa Y., Mitachi T., Itoh K. and Takashi K.: Possible use of Tilt-sensor for failure movement and failure plane just before slope failure, International Geotechnical symposium on “Geotechnical Engineering for disaster prevention and reduction”, Russia, 2007. (in print)

### 2. 国内学会・シンポジウム等

Tamrakar S. B., Toyosawa Y. and Kazuya I., Takashi K., Atsushi N. and Satomi O.: Development of Tilt-sensor and possibility of measurement of failure trend just before the failure, 第41回地盤工学研究発表講演集, 鹿児島, pp. 2253-2254, 2006.

小板橋拓馬, 末政直晃, 伊藤和也, Tamrakar S. B., 豊澤康男, 日下部澄音: 切土掘削工事中の斜面崩壊機構に関する実物大実験～試料の違いによる影響について～, 第 61 回土木学会年次学術講演集, pp. 381 - 382, 2006.

Tamrakar S. B., Toyosawa Y., Itoh K., Kunimi T., Nishijyo A, and Okubo T.: Comparison of slope failure trend just before failure in the field using newly developed tilt-sensor, 第 61 回土木学会年次学術講演集, pp. 433 - 434, 2006.

Timpong S., Tamrakar S.B., Toyosawa, Y. and Itoh K.: Deformation characteristics of sandy clay soil during slope excavation, 土木学会第 61 回年次学術講演集, III-267, pp. 529 - 530, 2006.

小板橋拓馬, 日下部澄音, Tamrakar Surendra B., 伊藤和也: 掘削に伴う斜面崩壊メカニズムの解明, 第 33 回土木学会関東支部技術発表会, III - 051, 2006.

日下部澄音, 小板橋拓馬, 伊藤和也, Tamrakar Surendra B.: 掘削に伴う斜面崩壊メカニズムの解明 (数値解析を用いて), 第 33 回土木学会関東支部技術発表会, III - 053, 2006.

Tamrakar S. B., Toyosawa Y. and Itoh K.: Development of Tilt-sensor for advanced prediction of failure and its applicability in the field excavation, 第 36 回安全工学シンポジウム, Vol. 36, 6-5, pp. 169 - 172, 2006.

Tamrakar S. B., Toyosawa Y., Itoh K. and Timpong S.: Relationship between critical failure height and trench excavation depth in relation to centrifuge tests performed with In-flight excavator, 第 36 回安全工学シンポジウム, Vol. 36, 6-6, pp. 173 - 176, 2006.

Timpong S., Toyosawa Y., Tamrakar S.B. and Itoh K.: Slope failure mechanism during Trench excavation in Peat, 第 36 回安全工学シンポジウム, Vol. 36, 6-7, pp. 177 - 178, 2006.

田中洋行・阿部篤史・笠間太樹・三田地利之: 「遠心力載荷実験による降雨時の斜面安定の検討」, 降雨時の斜面モニタリング技術とリアルタイム崩壊予測に関するシンポジウム, 鹿児島 (2006)

笠間太樹, 金子広明, 田中洋行, 工藤豊: 「遠心場における降雨再現実験での間隙水圧の挙動」, 地盤工学会北海道支部技術報告集, (47): 167-170 (2007)

久常雄大・大河原正文・三田地利之: 「原子間力顕微鏡による粘土の残留状態せん断面の表面粗さおよび摩擦力測定」, 地盤工学会北海道支部技術報告集, (46): 99-106 (2006)

大河原正文・三田地利之: 「粘土の残留状態におけるせん断抵抗係数  $\tan \phi' r$  と真実接触面積との関係」, 地盤工学会北海道支部技術報告集, (46): 107-114 (2006)

梅谷晋平・高橋秀彰・三田地利之: 「繰り返し一面せん断試験から求めた地すべり粘土の強度パラメータ」, 地盤工学会北海道支部技術報告集, (46): 139-140 (2006)

三田地利之：「粘土の残留強度と地すべり対策工設計用強度」，日本地すべり学会北海道支部特別講演，札幌（2006.4）

高橋秀彰・木崎健治・三田地利之・梅谷晋平・鈴木俊司・雨宮浩樹：「すべり面観察結果とせん断試験結果に基づく地すべり強度定数の評価」，第41回地盤工学研究発表会，鹿児島（2006）

梅谷晋平・高橋秀彰・三田地利之・田中洋行・齋藤和彦：「不攪乱・再構成試料による地すべり粘土の強度パラメータ算定例」，第41回地盤工学研究発表会，鹿児島（2006）

高橋秀彰・木崎健治・三田地利之：「泥岩および凝灰岩地すべりのせん断強度とすべり面粘土の特性」，第45回日本地すべり学会研究発表会，鳥取（2006）

梅谷晋平，高橋秀彰，三田地利之：「繰り返し一面せん断試験に基づく強度パラメータに及ぼす諸要因の検討」，地盤工学会北海道支部技術報告集，（47）：125-130（2007）

久常雄大，大河原正文，三田地利之：「原子間力顕微鏡による異なる温度条件下での高純度粘土の摩擦力・粘性係数測定」，地盤工学会北海道支部技術報告集，（47）：189-194（2007）

大河原正文，九千房修司，三田地利之：「残留状態せん断面のその場観察／分析用「小型せん断ユニット」の開発」，地盤工学会北海道支部技術報告集，（47）：195-198（2007）

## Failure heights comparison during excavation using in-flight excavator

S.B. Tamrakar, Y. Toyosawa, K. Itoh & S. Timpong

Construction Safety Division, National Institute of Industrial Safety, Tokyo, Japan

**ABSTRACT:** Normal and combination of normal and trench excavations were carried out for the statically compacted model slopes of Narita sand, Kanto loam and mixture of NSF clay and Toyoura sand using in-flight excavator. Normal excavation corresponds to the excavation made behind and above the toe level. Combined excavation corresponds to the toe excavation (excavation below the toe level) made at particular distance from the slope toe where normal excavation was already performed. In both types, excavation is continued until slope failure occurred and height of slope just before failure is calculated. Decrease in the failure height with an increase in trench excavation depth was observed in all types of soil models. Maximum failure height was observed during normal excavation. Whereas the combined excavation made near the slope toe showed the minimum failure height. Failure height increases with the increase in the distance of toe excavation from the toe. This might be due to extra increase in overburden pressure behind the cut. Image analysis of the photographs taken during the tests showed small movement with small and partial failure for Narita sand and Kanto loam and large movement with block failure for mixed soil. Sharp increase in the displacement values just before the failure measured at the slope crest showed the possibility of predicting failure in advance.

### 1 INTRODUCTION

Most of the accidents take place during the excavation of lower parts of the slopes, especially the trenches (excavation below the toe level). Earlier Tamrakar et al. (2005) carried out the tests at centrifuge using in-flight excavator for volcanic sand with and without making trench excavations at the beginning and it was reported that the vertical height before the failure was larger for the excavation made without trench at the start of trench excavation than the excavation made with the trench. In their research, only one type of soil was used and only two tests (with the trench excavation at the beginning or at the end) were performed. In this research, trench excavations are made at different distances from the toe of the slope along with the normal excavation and the effect of trench excavation on the failure height just before the failure was studied. Comparison of failure heights observed for the normal and combined excavations is made. With this, a better and safer position of trench excavation could be made. In-flight excavator which could be moved vertically up and down and horizontally left and right within the centrifuge environment is used for the excavation. At first, normal excavation was carried out until failure occurred. Then the distance from the toe of the slope to the failure position was noted. Finally, combination of normal and trench excavations were carried out within the distance measured earlier. In

this case, trench excavation was continued till the failure occurred. Finally, comparison of failure heights (height of the slope surface from the bottom line of excavation) for normal and combined excavations was made. Image analysis was also carried out by comparing the photographs taken at the start of excavation and just before the failure which shows the movement of soil mass behind the cut. Failure pattern of slope could be seen with this analysis. Deformation of top surface of the slope at each excavation was measured by setting up linear vertical differential transducers (LVDTs) on the slope top. Stepwise increment in the displacement with the progress of excavation was observed. LVDT set up closest to the crest showed the sharp increment just before the failure. This might be useful in predicting the failure in advance.

### 2 EXPERIMENTAL SETUP

#### 2.1 Preparation of model ground and model slope

In this experiment, three types of soil; Narita sand, Kanto loam and the mixed soil were used. First two soils were collected from the Toke excavation site, Chiba prefecture, Japan. Third soil was prepared in the laboratory by mixing NSF clay and Toyoura sand in the ratio of 1:3 by weight. Physical properties, particle size distribution and direct shear test results of these soils are shown in Table 1.

Accordingly, Narita sand is classified as SF (Sand with fines  $\leq 15\%$ ) and Kanto loam is classified as VH2-S (Volcanic sandy soil with liquid limit,  $w_L \geq 80\%$ ) (JGS0051-2000). Liquid limit and plasticity index of Kanto loam used are 129.3% and 38.1%, respectively. Soil specimens were thoroughly mixed with pre-determined water content ( $w$ ) and kept in plastic bag for several days. Model slope ground from these soils was prepared in a model box ( $0.45 \text{ m} \times 0.20 \text{ m} \times 0.272 \text{ m}$ ), by statically compacting them into number of layers using bellofragm cylinder. Model ground of Narita sand and mixed soil were prepared under 50 kPa where as model ground of Kanto loam was prepared under 25 kPa. Thickness of each layer is about 0.02 m and compaction time for each layer was about 5 minutes.

Once the compaction was completed, front and back panels of the model box were removed and model slope ground was then cut to required dimensions. Details of slope model are shown in Figure 1. Slope angle for each slope was fixed at 50 degree. This slope angle is lower than the one mentioned in the safety guideline

Table 1. Properties of soil specimens.

	Narita sand	Kanto loam	Mixed soil
$\gamma_s$ (kN/m <sup>3</sup> )	26.12	27.13	
$0.075 \times 10^{-3} \sim 2 \times 10^{-3} \text{ m}$ (%)	77.50	11.50	
$0.005 \times 10^{-3} \sim 0.075 \times 10^{-3} \text{ m}$ (%)	12.70	54.70	
$< 0.005 \times 10^{-3} \text{ m}$ (%)	9.80	33.80	
Avg. particle size, $D_{50}$ ( $\times 10^{-3} \text{ m}$ )	0.1909	0.0119	
Uniformity coeff., $U_c$	40.70		
Coefficient of Curvature, $C_c$	13.9		
Cohesion, $c$ (kPa)	9.78	6.12	16.80
Angle of internal friction ( $\theta^\circ$ )	15.88	40.05	16.68

$\gamma_s$  = unit weight of soil solids.

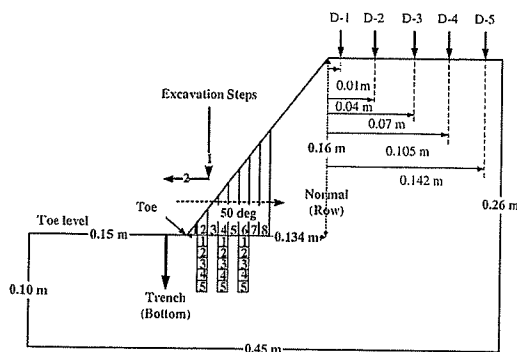


Figure 1. Outline of model slope showing the positions of LVDTs on the slope top.

of Labor Safety and Health Regulation. The lower and safer angle was selected so that longer slope length (i.e., distance of excavation from the toe of the slope) could be obtained which will facilitate to make trench excavations at different distances from the toe.

After making the model slope, side panels; with and without glass were attached to apparatus box in which model slope ground was made. In order to reduce the friction between the model ground and the model box panels, rubber membrane was placed in between. A thin film of silicon grease was applied between the membrane and the panels, which further reduces the friction. Lines (vertical and horizontal) were drawn on one side (glass) of the membrane so that it could be seen through the glass panel during the excavation. Later on, these lines were used to find the movement of the slope before and after the failure. Some parts of rubber membrane (from the toe to the distance at which the excavation was to be carried out) were cut into smaller pieces so that free movement of slope as well as clear excavation of each step could be commenced. The rubber membrane used has same size and shape as that of the model slope ground. Outline and final shape of the model ground are shown in Figure 1. Completed model slope along with model box was finally shifted to centrifuge platform. Direct contact type LVDT (D-1 to D-5) are placed on the top surface of the slope at 0.01, 0.04, 0.07, 0.105 and 0.142 m distances from the crest of the slope as shown in Figure 1. Once the set up of LVDT was finished, in-flight excavator was positioned in the centrifuge platform in such a way that its blade could move freely within the model box.

## 2.2 In-flight excavator

In-flight excavator developed by Toyosawa et al. (1998) shown in Figure 2 was used in this research.

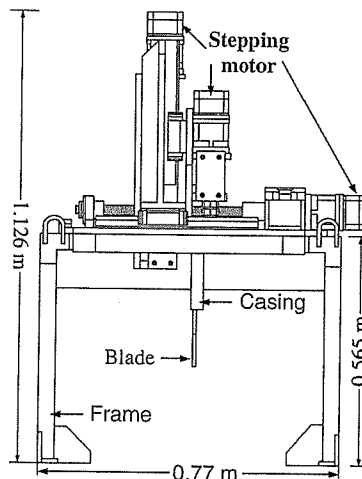


Figure 2. Outline of In-flight excavator.

This device is provided with a screw auger. Maximum rotation of the auger is 35 rpm and its ascent and descent speed is 0.005 m/sec and drifting speed is 0.005 m/sec. In this test, for the excavation, this auger is replaced by excavating blade of 0.2 m width. It could move up, down, left and right directions. Also, movement of blade in a horizontal direction makes it possible to shift away the excavated material smoothly from the slope. All the processes of excavation are controlled by 4 stepping motors. This in-flight excavator could be controlled manually or in semi-automatic way from the operating room.

### 3 DETAILS OF CENTRIFUGE MODEL TESTS

Bulk unit weight ( $\gamma_t$ ) and  $w$  for each test case of Narita sand and Kanto loam are shown in Tables 2 and 3, respectively. Experiments carried out for Narita sand

Table 2. Experimental conditions for Narita sand.

Type of excavation cases	Normal R-8-B-0	Combined R-2-B-5	Combined R-4-B-3	Combined R-6-B-2
$\gamma_t$ (kN/m <sup>3</sup> )	10.94	12.56	12.18	12.70
$w$ (%)	9.89	10.75	9.22	9.22
Centrifuge acceleration	31.3	31.3	31.6	31.8
Failure height (Row) (m)	2.985	0.746	1.507	2.275
Failure depth (Bottom) (m)	0	1.565	0.948	0.636
Real height at failure (m)	2.985	2.311	2.455	2.911
$H_{cr} = \{(4*c)/\gamma_t\}$ (m)	3.576	3.115	3.211	3.079

Table 3. Experimental conditions for Kanto loam.

Type of excavation cases	Normal R-7-B-0	Combined R-2-B-4	Combined R-4-B-2	Combined R-6-B-1
$\gamma_t$ (kN/m <sup>3</sup> )	8.93	9.00	9.02	8.95
$w$ (%)	91.68	91.11	90.17	88.16
Centrifuge acceleration	31.8	31.3	31.3	31.8
Failure height (Row) (m)	2.65	0.746	1.493	2.275
Failure depth (Bottom) (m)	0	1.252	0.626	0.318
Real height at failure (m)	2.65	1.998	2.119	2.593
$H_{cr} = \{(4*c)/\gamma_t\}$ (m)	2.742	2.721	2.119	2.593

and Kanto loam are mainly explained here. For both of these soils, one normal excavation and 3 combined excavations (normal + toe) were performed. One normal excavation test for mixed soil ( $\gamma_t = 14.94$  kN/m<sup>3</sup>,  $w = 9.65\%$ ) was also performed to compare the image analysis results of three types of soils during normal excavation failure.

Each excavation (cut) was carried out vertically downward and outward. In case of normal excavation, cutting was started from the slope surface to vertically downward and up to toe level. Width of each vertical cut of the model slope in normal excavation is 0.01 m. Each vertical cut (above the toe level) is represented by "Row (R)" and it is followed by the numbers as follows; R-1, R-2, R-3 and so on. R-1 represents the 1st cut, excavating at 0.01 m distance from the toe of the model slope. Similarly, R-2 and R-3 represent the second and third cuts, excavating the model slope at 0.02 and 0.03 m distances from the model slope toe, respectively. Combined excavation represents the trench excavation at particular normal cut (row). Trench excavation represents the vertical cut behind and below the toe level at particular R. Depth of each cut of trench of model is fixed at 0.01 m and trench excavation is represented by "Bottom (B)" which is followed by numbers as follows; B-1, B-2, B-3, and so on. B-1 represents the cut at 0.01 m below from the toe level. Similarly, B-2 and B-3 represent the cuts at 0.02 and 0.03 m depths from the model slope toe level, respectively.

Particular excavation might be either normal excavation or the combination of normal and trench excavations. Therefore, each case of excavation shown in Tables 2 and 3 is represented by the combination of normal (Row) and trench (Bottom) cuts. For example: R-2-B-5. This represents the width of normal cut behind and at the toe level is 0.02 m (i.e., at 0.02 m distance from the model slope toe) and depth of trench cut behind and below the toe level is 0.05 m; showing the excavation at 0.02 m distance from the toe and up to 0.05 m depth below the toe level. Similarly, R-8-B-0 represents the 8 cuts of "Rows", i.e., at 0.08 m distance from the toe. Here, B = 0 represents the excavation made without any trench excavations, i.e., only normal excavation.

In case of combined excavation, at first normal excavation was followed. Once the normal excavation reached the predetermined distance from the toe, trench excavation was followed. As mentioned earlier, depth of each bottom cut of trench excavation is 0.01 m. Two minutes interval was allowed after each bottom cut. Trench excavation was continued till the slope was failed. In Tables 2 and 3, excavation cases are named after the position of excavation where the slopes were failed.

In all the soil types, at first, normal excavation was carried out by cutting the slope behind the toe

in rows, until the slope was failed. In this type of excavation, cutting blade of excavator was vertically moved down from the slope surface and then moved outward horizontally when the blade reached the toe level of that cut. Two minutes interval time was allowed between each cut. Slope of Narita sand was failed at R-8-B-0. For Kanto loam and mixed soil, failure occurred at R-7-B-0. Combined excavation was carried at certain intervals within the distance of failure of normal excavation. Here, R-2, R-4 and R-6 were chosen to carry out the combined excavation.

In this research, height of the slope in the field from the toe level was assumed to be 5 m. In the model, height of the slope from the bottom of the model was 0.26 m and the height of the slope from the toe level was made 0.16 m. To make the slope height of 5 m, centrifuge acceleration was increased up to 31.3G. Similarly, for other cases also acceleration was fixed in such a way that the real height of the slope in the field becomes 5 m. Accelerations for each case are shown in Tables 2 and 3. During the centrifuge test, acceleration was increased gradually in steps from 5~10~15~20~25~31.3G. Once the vertical displacement become constant at 31.3G, then the excavation process was started.

#### 4 TEST RESULTS AND DISCUSSIONS

Excavation test results of Narita sand and Kanto loam are mainly discussed here. Critical failure height for each case of excavation failure is shown in Tables 2 and 3. In the table, all the values are changed into real field value by multiplying the data obtained from model test by the respective centrifuge acceleration values. "Failure height" in tables represents the height of slope above the toe level just before the failure. Similarly, "failure depth" represents the depth of trench cut below the toe level. "Critical failure height" is the summation of failure height and failure depth. "Critical height ( $H_{cr}$ )" shown in the Tables 2 and 3 was calculated theoretically by using the equation where bulk unit weight and cohesion are used. Critical heights calculated theoretically showed higher values than the critical failure height obtained for each test. In both Narita sand and Kanto loam, critical failure height obtained for the normal excavation case are very closer to critical height calculated whereas those obtained for the combined excavation cases, critical failure heights obtained are smaller than the critical heights calculated using the equation. Therefore, one should be careful while calculating the critical failure height during the combined excavation.

Figure 3 shows the failure height (Row) and failure depth (Bottom) just before the failure at particular distances of excavation from the toe. Excavation position (R-cut) of the model tests is multiplied by the

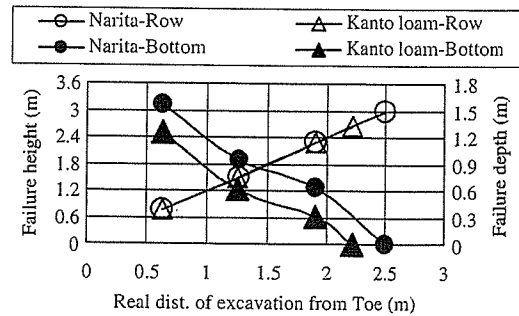


Figure 3. Failure height, failure depth and distance.

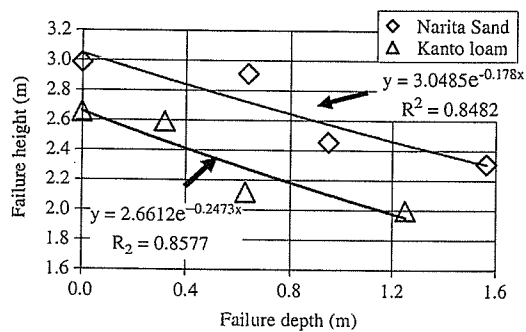


Figure 4. Relationship between failure height and failure depth.

centrifuge acceleration to get the real distance of excavation position from the toe. Non-linear decrease in failure depths with the increase in the real distance of excavation position is seen from the toe. This graph shows the inverse relationship between failure heights and failure depths with the increase in the position of distance of excavation from the toe. A non-linear relationship could be seen in case of failure depth. Graph shown in Figure 4 also shows the relationship between failure height and failure depth. Exponential regression lines shown in the figure could be used for predicting the probable failure height at particular depth of excavation. Figure 5 shows the non-linear relationship between critical failure height and real distance of excavation position just before the failure. From the graph, it could be observed that the critical failure height increases with the increase in the distance of excavation position from the toe. But the increment rate decreases with the increase in the excavation distance from the toe. This implies that at toe or near the toe, if the trench excavation is made, then the failure of slope occurs before it reaches the critical failure height that was obtained from the normal excavation. Henceforth, care should be taken while making the trench excavation.



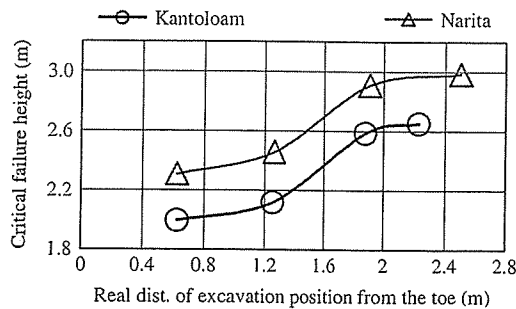


Figure 5. Real height and distance of excavation position from the toe just before the failure.

Decrease in the critical failure height with the increase in the failure depth (trench excavation) might be thought of due to the increase in the overburden pressure (weight of extra height) behind the cut. Generally, when the toe of the slope is excavated, shear strain is accumulated near the toe. With the advancement in the combined excavation steps near the toe, overburden pressure continues to increase. Continuous increment in the overburden pressure behind the cut increases the shearing strain which finally leads to failure and slope gets failed. This is the reason why critical failure height near the toe of the slope is smaller than those at farther distances from the toe. Therefore, for Narita sand and Kanto loam, critical failure height during R-2 cut shows the minimum value in comparison to R-7 and R-8 cuts where the critical failure heights have maximum values. From the results mentioned in Figures 2 to 5, it could be said that the maximum value of critical failure height could only be obtained for normal excavation cases and this critical failure height decreases with the decrease in the distance of excavation position as well as with the increase in the trench excavation depth.

The trend of increment of critical failure heights shown in Figure 5 for Narita sand and Kanto loam are similar. But the critical failure height obtained from the model test for Narita sand is higher than that for Kanto loam. This might be due to the effect of cohesion: Narita sand has higher cohesion value than Kanto loam (Table 1). Here, compaction pressure for Narita sand and Kanto loam were also different; Narita sand being prepared under 50 kPa and Kanto loam being prepared under 25 kPa. Except R-7-B-0 case of Narita Sand, in all the cases of Narita sand and Kanto loam soils, failure was partially occurred within the slope just behind the cut showing very small movement of soil masses behind the cut. But for mixed soil, large failure behind the cut with large movement soil mass in block behind the cut was seen. In order to check the movement of soil masses after the failure, image analysis was carried out from the photographs taken before the start of excavation and after the failure.

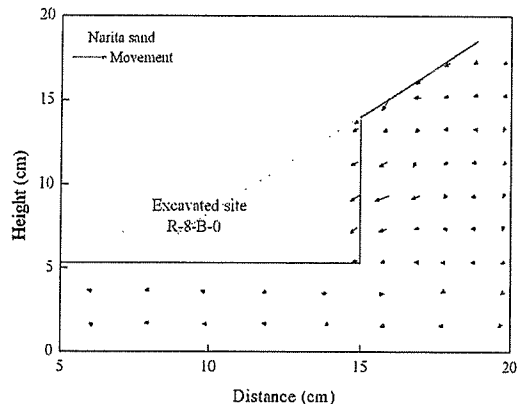


Figure 6. Movement at failure for Narita sand (R-8-B-0).

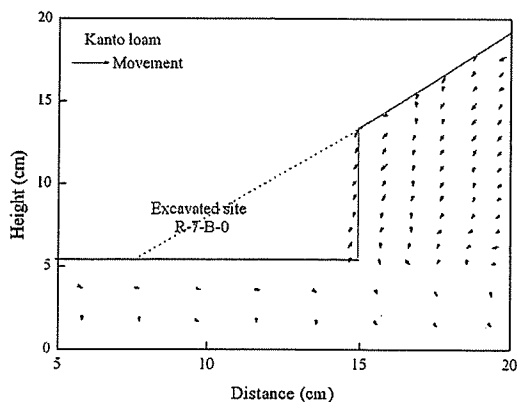


Figure 7. Movement at failure for Kanto loam (R-7-B-0).

Image analysis was done from the lines drawn on the rubber membrane. Figures 6, 7 and 8 show the relative movement of slopes before the start of excavation and just before the failure. It was found that the movement behind the cut before the failure was small for Narita sand and Kanto loam in comparison to mixed soil; mixed soil showing the maximum movement while Kanto loam showing the minimum movement.

Figures 9 and 10 show the vertical displacement measured from LVDTs set up on the top surface of the slope for normal excavation cases of Narita sand and Kanto loam, respectively. Bold vertical lines in the graph represent the steps of excavation. In both the graphs, gradual increase in vertical displacement with the increase in the steps of excavation could be observed. Comparing the amount of vertical displacement of each LVDT (D-1, D-2 and D-5), D-1 shows the maximum value and D-5 shows the minimum. This pattern of gradual decrease in vertical displacement shows the forward and downward movement of

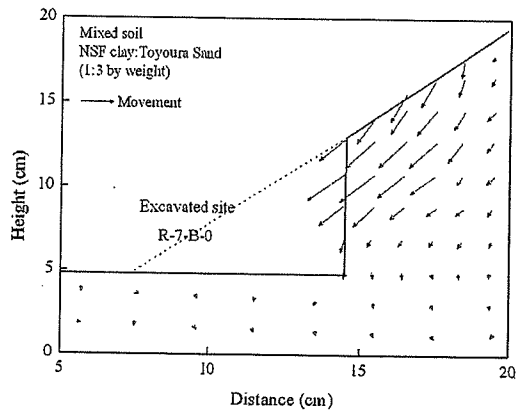


Figure 8. Movement at failure for mixed soil (R-7-B-0).

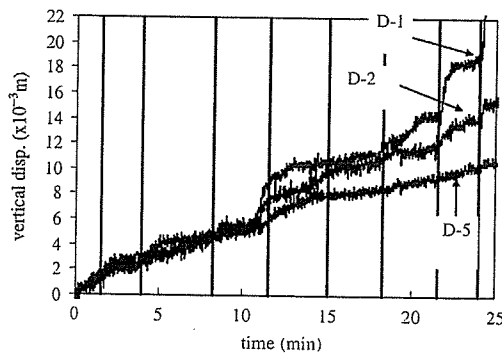


Figure 9. Vertical displacement with time (Narita sand).

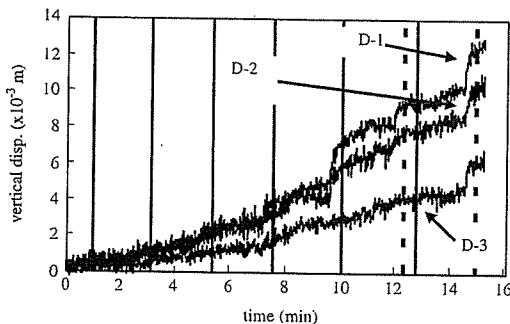


Figure 10. Vertical displacement with time (Kanto loam).

slope with the increase in excavation steps. Sudden increment of displacement just before the failure was seen for the LVDT (D-1) which is at the nearest distance from the slope crest. This sudden increase in the

displacement might be useful in predicting the possible failure.

## 5 CONCLUSIONS

- (1) Maximum critical failure height is obtained only for normal excavation. In case of combined excavation, critical failure height (failure height + failure depth) decreases with the increase in the trench excavation depth. Reduction in the critical failure height near and towards the toe is due to the increase in the overburden pressure (weight of extra height) behind the cut.
- (2) The trend of increment in critical failure height obtained for both Narita sand and Kanto loam are almost same. But the critical failure height obtained for Narita sand is higher than that obtained for Kanto loam. This might be due to cohesion values or compaction pressure used for preparing the soil.
- (3) From the image analysis, failure pattern or the movement of slope behind the cut could be observed. Partial failure and smaller movement behind the cut were seen for Narita sand and Kanto loam. Whereas larger and block movement were seen for mixed soil.
- (4) Gradual increment in vertical displacement measured on the top surface of slope showed the forward and downward movement of the slope. Sudden increment in vertical displacement, D-1 near the slope crest is helpful in predicting the failure.

## ACKNOWLEDGEMENT

This research is partially carried out under the Health and Labor Sciences Research Grants of Ministry of Health, Labor and Welfare, Japan.

## REFERENCES

- Japanese Geotechnical Society (JGS0051-2000). Methods of classification of Geomaterials for Engineering Purposes, *Soil testing methods and explanation*: 213-245.
- Tamrakar, S. B., Toyosawa, Y., Itoh, K. & Kusakabe, S. 2005. Failure mechanism of slopes in the centrifuge using In-flight excavator, *International symposium on Landslide Hazard in Orogenic Zone from the Himalaya to Island Arc in Asia*, Kathmandu, Nepal, 25-26 September 2005: 255-264.
- Toyosawa, Y., Horii, N. & Tamate, S. 1998. Deformation and failure behavior of anchored retaining wall induced by excessive excavation in centrifuge model tests, *Research Reports of the National Institute of Industrial Safety (NIIS-RR-97)*: 35-46.

## POSSIBILITY OF MEASUREMENT OF SLOPE MOVEMENT DURING THE SANDY SOIL SLOPE FAILURE IN CENTRIFUGE

Tamrakar Surendra Bahadur, Japan National Institute of Occupational Safety and Health, Tokyo, Japan

Toyosawa Yasuo, Japan National Institute of Occupational Safety and Health, Tokyo, Japan

Tanaka Hiroyuki, Hokkaido University, Hokkaido, Japan

Itoh Kazuya, Japan National Institute of Occupational Safety and Health, Tokyo, Japan

### ABSTRACT

Measurement of slope movement during the failure sandy slopes was studied by conducting manual excavations at the lower part of the slope in case of small size full scale tests and by in-flight excavations in case of centrifuge tests until failure occurred. Stepwise and sharp increment of slope movements of slope surface and slope top during and just before the failure with the elapsed time of excavation steps were seen in both the cases. Quick failure was seen for slopes which have higher slope angle and slope height in both the cases. Similar trends in measurement of all the instruments were seen. This showed the possible applicability of tilt sensors in the real field excavations. In centrifuge excavations, large deformation was seen near the slope crest. Limit equilibrium analysis was also carried out.

### RÉSUMÉ

La mesure du mouvement de pente pendant la chute des pentes arénacées a été étudiée en conduisant l'excavation manuelle à la partie inférieure de la pente en cas d'essai à grandeur nature de petit modèle et l'excavation en vol en cas d'essai centrifuge. Dans tous les deux cas, l'augmentation par degrés et brusque du mouvement à la surface et au sommet pendant et juste avant la chute a été observée, ainsi que la chute rapide pour les pentes qui ont un angle aigu et une hauteur élevée. On a observé une tendance semblable du changement des angles mesuré par le détecteur d'inclinaison et de la déformation mesurée par le détecteur de laser et le transducteur de déplacement vertical. Ceci a montré l'applicabilité du détecteur d'inclinaison dans un vrai chantier. En cas d'excavation centrifuge, une grande déformation a été observée près de la crête de pente. L'analyse d'équilibre de limite a été également effectuée.

### 1. INTRODUCTION

Slope failure due to the human induced construction works (excavation, embankment, etc.) sometimes takes the lives of the workers. In Japan, every year around 30 to 40 cases of such accidents are recorded. More than 50% of such accidents take place during the cutting or leveling the trench of lower part of slope. Slopes become safe only when they are excavated up to safe slope angle or some other protective works are carried out. But during excavation, slopes are at higher risk of failure. In many cases, without any prior signals of failure, instantaneous movement of slope occurs and the workers do not find sufficient time to escape and hence, accidents take place. To prevent such accidents, one should understand the failure mechanism. Also, it would be better if one could measure, predict and inform about trend of slope movement just before the failure.

In this research, failure mechanism of sandy slopes is studied by conducting small size full scale tests and centrifuge tests. For this, river sand was used. In case of small scale full size test, three tests were conducted by varying their slope angle from 50, 60 and 70 degrees along with slope heights varying from 1.3 to 2.2m for each slope angle. Manual excavation was made at the lower part of the slope (toe and trench excavations) until the slope get failed. Here, the trend of slope movement (degrees of movement and amount of deformation) were observed by

placing tilt sensors and laser sensors on the slope surface and on the slope top, respectively. In case of centrifuge tests, model slopes were prepared by static compaction within the apparatus box and cutting them into required dimensions. In this case also, three slope angles, 50, 60 and 70 degrees were used. They were then run into 6 and 10 time of gravity acceleration to obtain two slope heights. Vertical deformation of the model slope top was measured by linear variable differential transducers (LVDTs). In this case, excavation of lower part (toe and trench) of the model slopes were carried out by using in-flight excavator until failure occurred. Limit equilibrium analysis for the centrifuge model tests were also carried out to compare the failure pattern in the test and in the analysis.

Changes in the slope angle measured by tilt sensor and deformations measured by laser sensors placed on the slope top and slope surface due to excavation in case of small scale full size test showed similar trend. With the possible measurement of slope movement by tilt sensor during and just before the failure showed the possibility of using them in the real excavation field. In case of centrifuge, while comparing the deformation time graph, failure of slope occurred just after the larger deformations of the LVDT's placed near the slope crest, there by showing the most suitable place for deformation measurement. Limit equilibrium analyses were carried out for centrifuge model tests and factor of safety data were compared. Since the factor of safety for all the tests were around 1, it could be

said that centrifuge test results were appropriate.

2. EXPERIMENTS AND EXPERIMENTAL CONDITIONS

2.1 Small Size Full Scale Test and Instrumental Set Up

In order to carry to out the small size full scale test in the laboratory, a full scale test box was made. Framework of the test box is constructed from the wooden planks, which are supported externally by the iron plates/beams. Frameworks shown in Photo 1 are used. Framework has two sections; lower cross section is 1.35m x 2.7m with 1.3m height and upper cross section is 1.35m x 1.2m with 0.9m. For smaller height slopes, only frontal section is used so that the total slope height is almost equal to 1.3m. In this case, weight of material in the upper section behind the slope might affect the failure movement of frontal section. Layout of small height model is shown in Fig. 1(a). For larger slope height, whole the height of the box is used so that the total height of the slope becomes almost equal to 2.2m. Outline of such model is shown in Fig. 1(c). Base of the box (slope) is 0.3m. Hence the slope heights for small and large slopes become 1m and 1.9m.

River sand was used as the test material. Here, medium dense test model was tried to obtain. Manual compaction was done in layers by spreading and tamping the sand with small wooden planks. Once the compaction was over, wooden planks of the front as well as side faces of model box were removed and cutting of slopes were done so that the test model of desired slope angle and slope height could be obtained. With three slope angles (50, 60 and 70 degrees) and two slope heights (1m and 1.2m), in total six tests were conducted. Water content and bulk unit weight of each test are shown in Table 1. Outline of model slopes are shown in Figs. 1(a), (b) and (c).

Once the desired slope of the test model was ready, then the set up of measuring instruments was done. Three types of measuring instruments were used; laser sensor, direct vertical displacement transducers (VDTs) and tilt sensor. First two instruments were used to measure the deformation of slope surface and slope top (vertical) where as the third instrument was introduced to measure the change in the angle due to the movement of slope surface and deformation of the slope top due to excavation. Tilt sensor is an acceleration sensor which is made in such a way that its output voltage could be changed into the tilt angle. Tilt sensor used in this research is shown in Photo 2. This could measure the angles in both X and Y directions with possible measurement of positive and negative angles. It's measuring range is  $\pm 20^\circ$  with sensitivity of 100mV/deg. This tilt sensor could also be used a thermo sensor. But this facility was not used in the tests here as tests were conducted inside the laboratory where temperature is considered to be constant.

Photo 1. (a) Lower section and (b) Whole framework

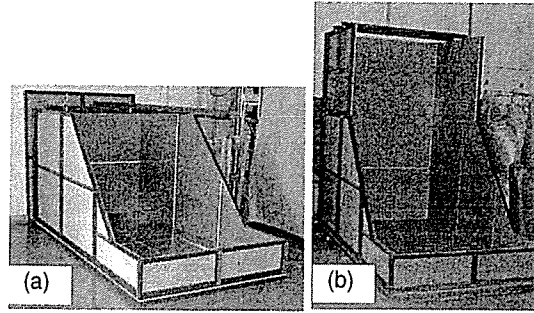


Figure 1. Outline of Small scale full size tests (a) for Slope-I-2, (b) for Slope-IV-1, Slope-V-2 and (c) for Slope-II-3, Slope-IV-2, Slope-V-2

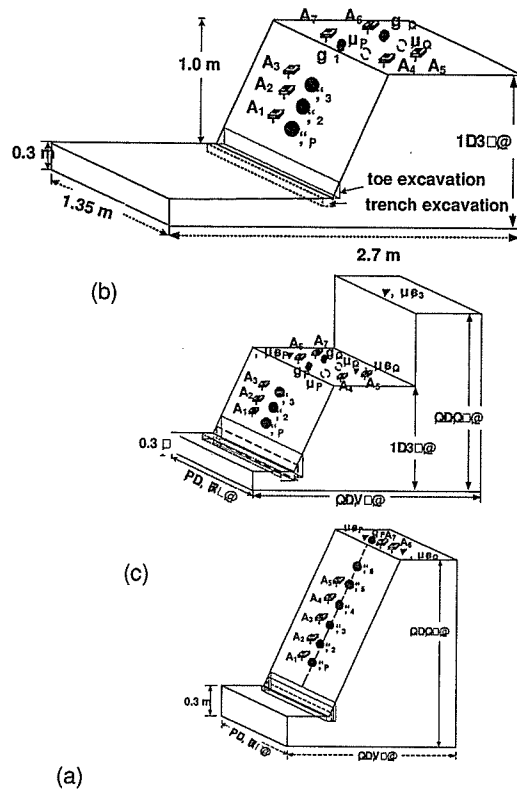


Table 1. Experimental conditions.

Test	Slope Angle	Water Content (%)	Unit Weight $kN/m^3$	Failure	
				Steps	Time min.
Slope-I-2	50	8.05	13.78	5	33.5
Slope-II-3	50	8.54	14.69	2	6.5
Slope-IV-1	60	7.55	15.30	13	99.6
Slope-IV-2	60	7.55	15.30	8	51.0
Slope-V-1	70	7.00	15.48	21	192
Slope-V-2	70	7.00	15.48	7	46.8